

Title	Study of Beam Profile Monitor for the Proton Linac
Author(s)	Shirai, Toshiyuki; Dewa, Hideki; Iwashita, Yoshihisa; Okamoto, Hiromi; Fujita, Hirokazu; Kakigi, Shigeru; Noda, Akira; Inoue, Makoto
Citation	Bulletin of the Institute for Chemical Research, Kyoto University (1993), 71(1): 15-20
Issue Date	1993-03-31
URL	<a href="http://hdl.handle.net/2433/77495">http://hdl.handle.net/2433/77495</a>
Right	
Type	Departmental Bulletin Paper
Textversion	publisher

## Study of Beam Profile Monitor for the Proton Linac

Toshiyuki SHIRAI\*, Hideki DEWA\*, Yoshihisa IWASHITA\*,  
Hiromi OKAMOTO\*, Hirokazu FUJITA\*, Shigeru KAKIGI\*,  
Akira NODA\* and Makoto INOUE\*

*Received February 9, 1993*

We have constructed a beam profile monitor for the ICR proton linac. A fluorescent screen is used to detect the proton beam. The material of the screen is an alumina ceramic doped with the chromium oxide and suitable for the beam monitor. The fluorescence is observed by a CCD camera and digitized by an image freezer. We have already used the profile monitor for the adjustment of the beam transport system. It is tested to be used as an emittance monitor.

KEY WORDS: Beam profile monitor/ Fluorescent screen/ Linac

### 1. INTRODUCTION

In an accelerator, a beam profile monitor is an important device to show a charged particle distribution in a beam. In our linac, which is composed of a 50 keV  $H^+$  ion source, 2 MeV RF-Quadrupole (RFQ) linac and 7 MeV Alvarez linac,<sup>1)</sup> 4 fluorescent screens (Desmarquest, AF995R) for the beam profile monitors are placed. The locations are shown in Fig. 1. It is also planned to be placed downstream to monitor the output beam of the Alvarez linac. The major role of the fluorescent screens from 1 to 3 is to help the adjustment of the focusing parameters for the optimum injection into the RFQ.<sup>2)</sup> The information of the beam injection into the RFQ and the RFQ cavity itself can be obtained by the beam profile on the screen 4.

Other kinds of profile monitors are known, such as a multi-wire current sensor and an electrostatic pick up of beam-induced signals. The latter is an attractive, because it does not destruct the beam. On the other hand, the fluorescent screen has a unique feature. It is a good resolution of the position. Because the resolution is limited by the multiple scattering of the injected beam and the range is short. The structure of the detector is simple compared to other monitors, which increases the reliability of the monitor.

A schematic diagram of the profile monitor is shown in Fig. 2. The fluorescent screen is attached to the movable cylinder and can be placed in the beam axis. The fluorescence is observed by a CCD (charge-coupled device) camera (PULNIX model TM720) which is placed 80 cm away from the axis. The output signals from the CCD are digitized and stored by image freezer. The digitized image is displayed on a TV monitor and transferred to a computer. The detailed information such as an intensity distribution is displayed on the monitor of the computer.

\* 白井敏之, 出羽英樹, 岩下芳久, 岡本宏巳, 富士田浩一, 柿木 茂, 野田 章, 井上 信: Nuclear Science Research Facility, Institute for Chemical Research, Kyoto University.

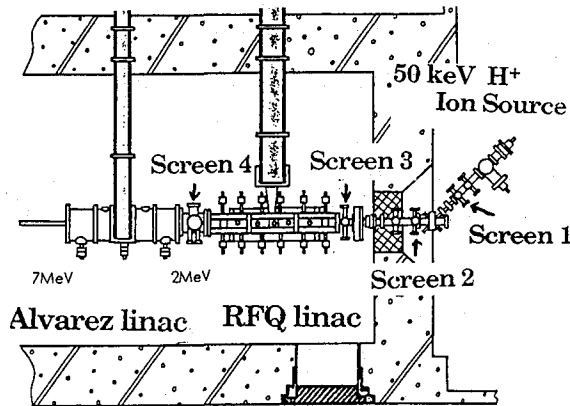


Fig. 1. Locations of the fluorescent screen for the beam profile monitor in the beam line of the ICR linac.

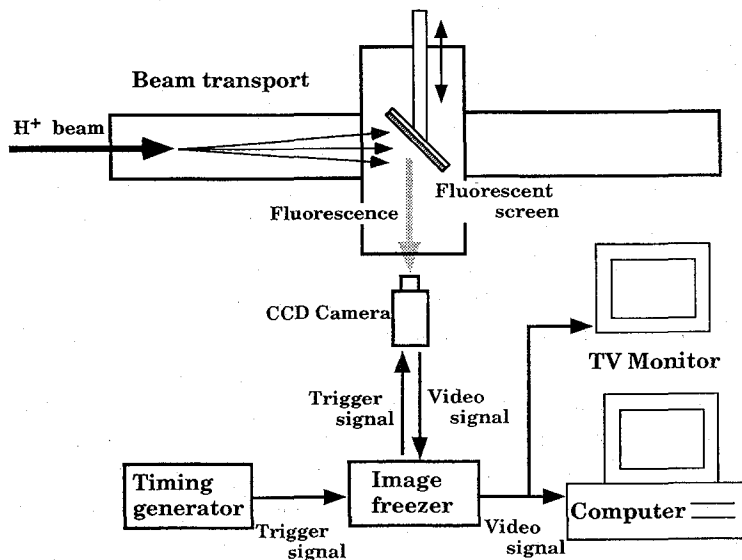


Fig. 2. Schematic diagram of the beam profile monitor system.

## 2. FLUORESCENT SCREEN

The assembled screen is shown in Fig. 3. The area of the fluorescent screen is  $50 \text{ mm} \times 50 \text{ mm}$  and the thickness is  $1 \text{ mm}$ . The fluorescent material is an alumina ceramic ( $99.5\% \text{-Al}_2\text{O}_3$ ) in which a little chromium oxide is homogeneously doped. The material has a high resistance against a radiation damage and a high temperature caused by the beam, which are suitable characteristics as the beam profile monitor.

The change of the vacuum pressure is less than  $1 \times 10^{-7}$  torr by the beam irradiation on the screen. It is an advantage for using it near an accelerator cavity. The life time of the screen is

Study of Beam Profile Monitor for the Proton Linac

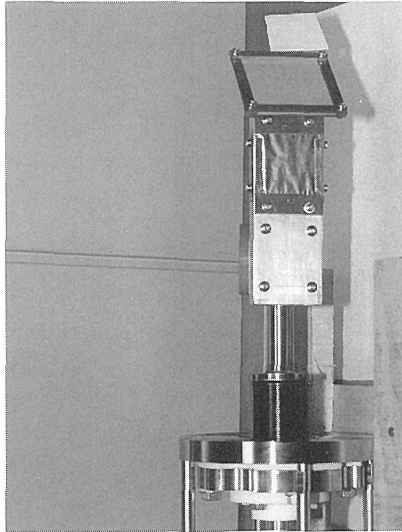


Fig. 3. Fluorescent screen assembly. The screen is attached at the end of the movable cylinder.

reported to be  $10^{18}$  electrons/mm<sup>3,2)</sup> But the surface of the screen changed to a metallic color and the light intensity decreased in our experiment. We suppose that a stainless mesh that was put on the screen surface to avoid discharging, was sputtered by the beam onto it. The screen without mesh sheet is now under the test.

The spectrum of the fluorescence were measured at screen 3 by 50 keV proton beam and at screen 4 by 2 MeV beam. A monochromator (SHIMADZU model SPG100ST) and a PMT (photo multiplier tube, HAMAMATSU model R928-09) were used for the measurement. The results are shown in Fig. 4(a) and (b). There are multiple peaks in the Fig. 4(a). It suggests that the multiple different processes of the fluorescence exist. The major peak is at 696 nm that is independent on the beam energy. It is major light source as the profile monitor and the

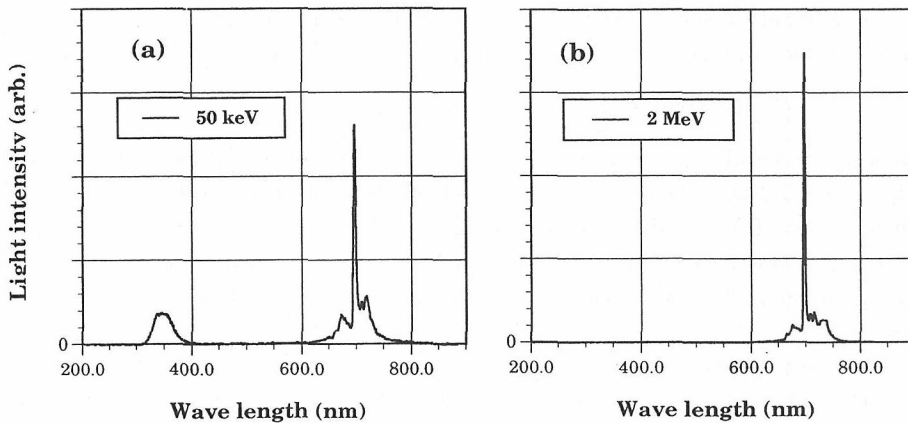


Fig. 4. The spectrum of the fluorescence of the screen : (a) the beam energy is 50 keV and the current is 200  $\mu$ A, (b) the beam energy is 2 MeV.

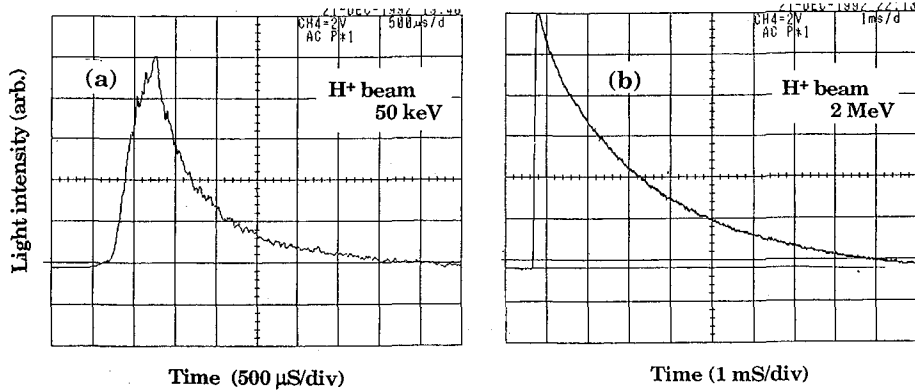


Fig. 5. The residual of the fluorescence of the screen : (a) the beam energy is 50 keV and the current is 200  $\mu$ A, (b) the beam energy is 2 MeV.

insertion of the filter to cut other peaks is planned to reduce the noise.

The residual of 696 nm fluorescence is shown in Fig. 5(a) by 50 keV beam and (b) by 2 MeV beam. The lifetime is 450  $\mu$ sec and 2.5 msec, respectively. The rise time of the signal in the Fig. 5(a) is determined by the per-amplifier, not by that of the fluorescence itself.

### 3. CCD CAMERA

The image on the screen is viewed by the CCD camera. The effective number of the CCD elements is 512 $\times$ 247 in the CCD camera. The total resolution in the system is limited by that of the video camera to observe the fluorescence in addition to that of the screen. The vertical resolution of the camera is 0.2 mm/element and the horizontal one is 0.1 mm/element.

The linac is operated in pulse mode. The pulse width is 50  $\mu$ sec and the repetition is variable from 0.5 Hz to 180 Hz. Because the shutter timing of the CCD camera must be synchronized to that of the linac operation, it should be controlled by an external trigger. The trigger is generated from the master trigger signal of the linac operation. The shutter speed is at 1 msec, which is close to the life of the fluorescence. The stop of the camera is determined so that the CCD output should not be saturated at the maximum beam current.

The relation between the input light intensity ( $I$ ) and CCD output voltage ( $E$ ) is,

$$E = cI^\gamma \quad (c: \text{constant}).$$

The value of  $\gamma$  is usually chosen to be 0.45. It is useful from a point of the wide dynamic range but the quantizing noise becomes large. We chose the camera of which  $\gamma$  was 1.0. The measured results of the relation is shown in Fig. 6. The amount of the light was varied by changing the shutter speed. It can be well fitted by the linear function but it does not pass through the origin. The measured beam profile data have to be calibrated by the obtained relation.

There are some factors of measurement errors in the CCD camera. When the beam profile is measured with the fast shutter speed mode (30  $\mu$ sec), the vertical smearing become severe. We chose the interline transfer CCD to have very little smearing but it does not free from it. On the other hand, when the light source is too bright, the blooming occurs and the image is enlarged

## Study of Beam Profile Monitor for the Proton Linac

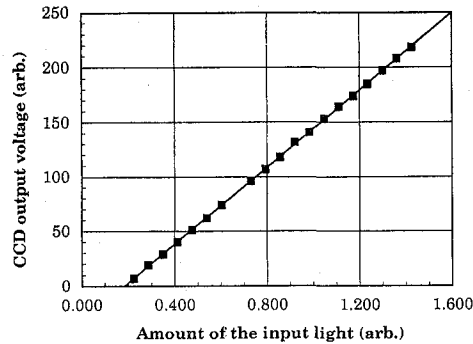


Fig. 6. The relation between the input light intensity and the CCD output voltage. The line is fitted linearly.

than real one.

The test was carried out in the following way. The images of the small spot were taken by the camera at the shutter speed, 1 msec and 30  $\mu$ sec and of the different stop size. In the results, the smearing is not found in the fast shutter mode. As for the blooming, the size of image is independent on the stop size at the 1 msec shutter speed unless the CCD output is saturated. But the image size at 30  $\mu$ sec shutter speed has the dependence and it is 5% larger than that of at 1 msec shutter speed. The precise measurements are difficult in the fast mode. An external shutter may be necessary before the camera.

The radiation and the electromagnetic noise also may cause noises on the CCD output signal. The video signals in our camera are noisy at first. It can be removed perfectly by an electromagnetic shield. The effect of the radiation is not seen but it must be tested by a long term operation.

The CCD output signals are digitized with 256 steps by the image freezer and the digitized image are held in the memory until the next external shutter trigger enters. The froze image is displayed on the TV monitor and the video signals are also transferred to the computer (NEC model PC9801VX) through an interface board. The intensity is calibrated by the result of Fig. 6 and the final image displayed on the monitor of the computer.

### 4. BEAM PROFILE AND THE EMITTANCE

Figure 7 shows the example of the beam profile at the downstream monitor of the RFQ (screen 4). The distance between the RFQ vane end and the screen is 495 mm. The beam energy is 2 MeV and the beam current is 400  $\mu$ A. The beam size is consistent with a result of the particle tracking simulation by the PARMTEQ code.<sup>4)</sup>

The transverse emittance can be measured by the fluorescent screen and movable slits. The emittance is a quantity to show the particle distribution in the phase space. The slits define the transverse position and spread of the beam. The transverse momentum can be measured by the screen that is located at the downstream of the slits. Because of the high position sensitivity of the screen, we can get the high resolution of the transverse momentum. The solid line in Fig. 8 shows the measured unnormalized emittance (90% value) in the  $x-x'$  phase space at the downstream of the RFQ. It is  $32.5 \pi$ -mm-mrad at the beam energy of 2 MeV and the total beam current of 400  $\mu$ A. The dotted line shows a simulation result by the PARMTEQ code.

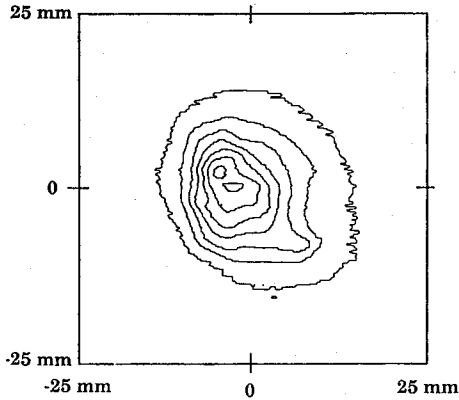


Fig. 7. Beam profile at the downstream of the RFQ. The beam energy is 2 MeV and the current is 400  $\mu$ A.

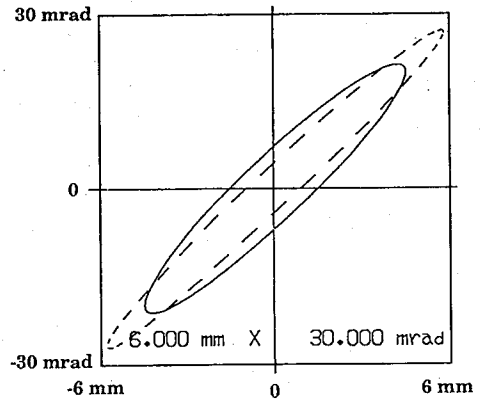


Fig. 8. Beam emittance at the downstream of the RFQ. The measured one (solid line) and the simulated one by the PARMTEQ code (dotted line). The beam energy is 2 MeV and the current is 400  $\mu$ A.

## 5. CONCLUSION

We have developed the beam profile monitor that consists of the fluorescent screen, the CCD camera and the image freezer. The beam profile has been measured successfully and it helps the operation of the linac.

The present screen material has a long lifetime of the fluorescence. It is convenient for the CCD camera, because its shutter speed is slow. But it is not adequate to measure the change of the beam profile or the emittance within a beam macro pulse. The material which has a fluorescence of a short lifetime is desirable for the purpose. We are looking for the new material for the screen.

As for the adjustment of the beam transport, the information is needed of not only the beam profile, but also the twiss parameter. It can be measured if the profiles are measured at the different upstream quadrupole strength.<sup>5)</sup> The test is planned.

## ACKNOWLEDGEMENT

The authors would like to thank Dr. Muto (INS) especially for his suggestion about the CCD camera. We thank the staff of the TAKENAKA SYSTEM Co., Ltd. and the SHIMADZU Co., Ltd. for their technical advices.

## REFERENCES

- (1) Y. Iwashita, et al., "System of 7 MeV Proton Linac", *Bull. Inst. Chem. Res., Kyoto Univ.*, **68**, 156 (1990).
- (2) A. Noda, et al., "Characteristics of the Ion Source and Low Energy Beam Transport of the Proton Linac at ICR", *Bull. Inst. Chem. Res., Kyoto Univ.* **71**, 6 (1993).
- (3) Y. Hashimoto, et al., "Beam Profile Monitor Using Alumina Screen and CCD Camera", *Proc. of the 7th Symp. on Accelerator Sci. and Tech., Saitama, Japan*, 314 (1991).
- (4) K.R. Crandall, et al., "RF-Quadrupole beam dynamics design studies", *Proc. of the Linear Accelerator Conference, Los Alamos*, 205 (1990).
- (5) O. Kester, et al., "Beam Emittance measurement from CERN Thermionic Guns", *Proc. of the European Particle Accelerator Conference, Berlin*, 1017 (1992).